PCCP

Effect of aromatic ring fluorination on CH…π interactions: Microwave spectrum and structure of the 1,2-difluorobenzene…acetylene dimer

Journal:	*Physical Chemistry Chemical Physics*
Manuscript ID	CP-ART-07-2016-004737.R1
Article Type:	Paper
Date Submitted by the Author:	03-Aug-2016

Complete List of Authors:	Akmeemana, Anuradha; Eastern Illinois University, Chemistry Kang, Justin; Oberlin College, Department of Chemistry and Biochemistry Dorris, Rachel; Eastern Illinois University, Chemistry Nelson, Rebecca; Eastern Illinois University, Chemistry Anderton, Ashley; Eastern Illinois University, Chemistry Peebles, Rebecca; Eastern Illinois University, Chemistry Peebles, Sean; Eastern Illinois University, Chemistry Seifert, Nathan; University of Virginia, Chemistry Department Pate, Brooks; University of Virginia, Chemistry Department

Effect of aromatic ring fluorination on CH…π interactions: Microwave spectrum and structure of the 1,2-difluorobenzene…acetylene dimer

Anuradha G. Akmeemana,[a] Justin M. Kang,[b] Rachel E. Dorris,[a] Rebecca D. Nelson,[a] Ashley M. Anderton,[a] Rebecca A. Peebles,[a] Sean A. Peebles,*[a] Nathan A. Seifert,[c] Brooks H. Pate[c]

[a] Department of Chemistry, Eastern Illinois University, 600 Lincoln Avenue, Charleston, IL 61920, USA

[b] Department of Chemistry and Biochemistry, 119 Woodland Street, Oberlin, OH, 44074, USA

[c] Department of Chemistry and Biochemistry, University of Virginia, McCormick Road, PO Box 400319, Charlottesville, VA 22904, USA

Keywords: o-difluorobenzene, rotational spectrum, van der Waals, weak hydrogen bonding

Electronic Supplementary Information (ESI) available: *Ab initio* results for MP2 and DFT predictions of the higher energy planar form of 1,2-difluorobenzene…acetylene, rotational transition frequencies for all isotopologues, principal axis coordinates for the r_0 experimental fit and BSSE corrected ωB97X-D optimizations with aug-cc-pVDZ basis set.

* Corresponding author. Email: sapeebles@eiu.edu, Tel: (217) 581-2679

Abstract

Rotational spectra for the normal isotopic species and for six additional isotopologues of the 1,2-difluorobenzene…acetylene ($C_6H_4F_2$…HCCH) weakly bound dimer have been assigned in the 6–18 GHz region using chirped-pulse Fourier-transform microwave spectroscopy. This is the third complex in a series of fluorinated benzene…acetylene dimers. In 1,2-difluorobenzene…HCCH, the H…π distance (2.725(28) Å) is longer by about 0.23 Å, and the estimated binding energy (E_B = 2.3(6) kJ mol^{-1}) is weaker by about 1.8 kJ mol^{-1}, than in the previously studied fluorobenzene…HCCH complex. In addition, in 1,2-difluorobenzene…acetylene, HCCH tips ~46(3)° away from perpendicular to the aromatic ring, with the H nearest the ring moving away from the fluorine atoms along the C_2 axis of the monomer, while in the fluorobenzene and benzene complexes HCCH is perpendicular (benzene…HCCH) or nearly perpendicular (fluorobenzene…HCCH, ~7° tilt) to the ring plane. Results from *ab initio* and DFT calculations will be compared to an experimental structure determined from rotational constants for the DCCD and five unique ^{13}C substituted isotopologues.

1. Introduction

CH…π interactions are a category of weak intermolecular forces that has increasingly been shown to be significant in a broad range of chemical applications, including biochemical systems, supramolecular chemistry, and structures of natural products. An excellent database of papers demonstrating the wide variety of research areas in which CH…π interactions play an important role may be found on Nishio's web site, *The CH/π hydrogen bond*.[1] The significance of CH…π interactions in biochemistry is highlighted in a recent study by Kumar, who showed,

in a search of the full set of polypeptide chains in the Protein Data Bank, that a significant fraction (roughly 15-20%) of residues participates in CH…π interactions.[2] Such noncovalent interactions are important in guiding structure and function of biomolecular systems, and both experimental and theoretical information are required to help generate and test viable theoretical models (e.g. force fields[3]) to examine and probe the nature of such weak interactions in protein structure and other applications. Recently, we presented rotational spectroscopic studies of benzene(BZ)…HCCH[4] and fluorobenzene(FBZ)…HCCH,[5] and we now use Fourier-transform microwave spectroscopy and *ab initio* calculations to extend this series of dimers to the first difluorobenzene complex with HCCH: 1,2-difluorobenzene(1,2-DFBZ)…HCCH.

BZ…HCCH4 and FBZ…HCCH5 have minimum energy structures in which HCCH is located above and perpendicular (BZ…HCCH) or nearly so (FBZ…HCCH) to the ring, with an H…π distance of about 2.492 Å in both dimers. In the FBZ complex, the end of HCCH nearest FBZ tilts slightly away from fluorine. The microwave studies indicated a decrease in binding energy of about 3 kJ mol^{-1} between the BZ and FBZ complexes (from 7.1(7) kJ mol^{-1} to 4.1(8) kJ mol^{-1}, based on a pseudodiatomic approximation). Mishra, *et al*[6] have compared methyl- and fluoro- substituted benzenes, and their results indicate that the trend in binding energies may be related to the activating or deactivating properties of aromatic ring substituents (although theoretical results give overall larger binding energies and typically focus on nonpolar fluorobenzenes).6 For more acidic (activated) CH bonds, a larger electrostatic component is expected, while weaker CH…π interactions tend to show a much more significant contribution from dispersion.[7,8] For instance, for benzene(BZ)…HCCH, an energy decomposition analysis puts the dispersion contribution at more than three times the size of the electrostatic contribution[9] (unfortunately, similar calculations have not yet been performed for the FBZ or 1,2-DFBZ

analogs with HCCH). A theoretical study focusing on Ar complexes of BZ, FBZ and 1,4-DFBZ revealed almost identical binding energies in all three cases, since a reduction of destabilizing effects resulting from contraction of the π electron density was largely canceled by a decrease in stabilizing contributions resulting from polarization related effects.[10]

Systematic substitution of an element such as fluorine in place of aromatic H atoms leads to a wide variation in electric dipole and quadrupole moments of the aromatic molecules. These variations may also lead to differences in the balance of dispersion and electrostatic forces as the degree and position of ring fluorination is varied. Previous papers on microwave spectra of BZ…HCCH4 and FBZ…HCCH5 complexes provide a more thorough summary of theoretical literature and other spectroscopic studies on HCCH···aromatic and related complexes.

There are few previous rotational spectroscopic studies on the effect of aromatic ring fluorination on intermolecular interactions. In one recent related study, Caminati *et al.* contrasted pentafluoropyridine…H_2O with pyridine…H_2O.[11] They showed that in pentafluoropyridine…H_2O the fluorine atoms draw sufficient electron density out of the aromatic ring to form a "π-hole" with which one of the lone pairs from the water molecule interacts. In contrast, H_2O interacts with pyridine *via* a hydrogen bond to the nitrogen atom, with one H–O bond of water lying in the plane of the aromatic ring. (High resolution spectroscopic results for pyridine…H_2O have not, to our knowledge, been published, but theoretical and matrix isolation infrared studies provide evidence of the near-planar structure of pyridine…H_2O.[12,13,14]) The series of hydrogen halides with BZ has average C_{6v} symmetry,[15,16,17] and in analogy to the HCCH complexes, adding one fluorine atom to the aromatic ring, for FBZ…HCl, leads to a tilt of the H–Cl axis towards the *para* position of the ring.[18] For both HCl and HCCH complexes, *ab initio* minima were found corresponding both to H…π bonded and planar or near-planar H…F

bonded structures. For FBZ…HCl, only the H…π structure was stable following basis set superposition error (BSSE) corrections,[18] while for FBZ…HCCH the planar CH…F configuration was less stable by >150 cm^{-1} at both BSSE corrected and uncorrected levels (although with a larger basis set than the HCl calculations).5 It will be interesting to investigate whether the "tilt" of HCCH away from perpendicular in the C–H…π structures continues to increase as molecular moments vary with addition of fluorine atoms, and whether a sufficient degree of ring fluorination ultimately leads to a change in observed HCCH (or HX) position to lie within, rather than above, the aromatic ring plane. This type of change in complexation mode was experimentally observed for water complexes, where H_2O forms a hydrogen bond to fluorine in the plane of the aromatic molecule for FBZ… and 1,4-DFBZ…H_2O,[19] but a π hydrogen bonded structure with H_2O above the ring is observed for BZ…H_2O.[20,21]

2. Computational and Experimental Methods

2.1 Ab initio calculations

Initial optimizations of plausible structures for the 1,2-difluorobenzene…acetylene complex (with acetylene in numerous different orientations either above the aromatic ring or in the ring plane) were carried out using the Gaussian 09[22] suite of programs, providing rotational constants to guide spectroscopic assignment. The MP2 level with a 6-311++G(2d,2p) basis set, which has been successfully used for predictions of other members in this series,[4,5] did not prove as helpful in the present case. With default optimization criteria, the resulting stationary points for the non-planar forms were found to depend heavily on starting orientation, with a variety of tilts of HCCH with respect to the ring being observed, the potential energy surface (PES) apparently being quite flat in the region of the minimum. Values of dipole moment components

and rotational constants are sensitive to this variation and the spacing and relative intensities of the transitions used to identify the spectrum can therefore vary considerably. Difficulties encountered in spectral assignment (discussed further in Section 3.1) and our initial belief that the spectrum might be displaying effects of some sort of internal motion led us to explore more cost effective density functional theory (DFT) methods. The M06-2X[23] and ωB97X-D[24] functionals were selected for their demonstrated performance in describing non-covalent interactions (see for example, ref. 6, which focuses specifically on interactions of HCCH with substituted (non-polar) benzenes). These functionals provide a less resource-intensive approach than MP2, making anharmonic frequency calculations (to predict centrifugal distortion constants) or PES scans (to identify possible tunneling pathways) feasible. MP2 and DFT optimizations were carried out with and without BSSE corrections using the Boys-Bernardi counterpoise approach,[25] and with different basis sets (Pople's 6-311++G(2d,2p) (492 primitive Gaussian functions) and Dunning's augmented correlation consistent aug-cc-pVDZ (496 primitives) and aug-cc-pVTZ (882 primitives)). The aug-cc-pVTZ basis set proved too large to permit a practical calculation of the BSSE optimized geometry so its use was not pursued further.

2.2 Microwave spectroscopic measurements

We first attempted to identify the 1,2-DFBZ…HCCH spectrum on our 480 MHz chirped-pulse FTMW spectrometer at Eastern Illinois University (EIU)[26] using data compiled from a 5,000 free induction decay (FID) average over each 480 MHz segment of spectrum between ~8-13 GHz. Samples of 1% of each component (1,2-DFBZ, 98%, Aldrich; HCCH, welding grade, Gano Welding Supply, Charleston, IL), diluted in He/Ne (17.5% : 82.5%, BOC Gases) were delivered to the nozzle at a pressure of 2 atm and at a nozzle pulse rate of 2 Hz. These scans were unsuccessful, since very few transitions remained after known monomer and dimer species

were eliminated. Due to the low intensity of these transitions, a more deeply averaged scan was sought. Given that compiling many hundreds of thousands of averages over a several gigahertz region with our own reduced bandwidth CP-FTMW spectrometer is not practical, a search was initiated at the University of Virginia using the 11 GHz bandwidth instrument.[27] A sample mixture of 0.1% 1,2-DFBZ and 0.25% HCCH (>99%, Praxair) diluted in Ne at a pressure of 1.3 atm was expanded simultaneously through 4 nozzles into the vacuum chamber. A total of 1.1 million averages was compiled, with 10 FIDs collected per gas pulse, at a nozzle repetition rate of 3.33 Hz.

A resonant cavity FTMW spectrometer of the Balle-Flygare design[28] located at EIU[29] was used to make additional measurements of weaker transitions and also those of isotopic species. A second broadband scan, from 6 − 20 GHz, consisting only of 0.2% 1,2-DFBZ in Ne (this time using 5 nozzles for a total of 500,000 FIDs averaged) was obtained at a later date from UVa and was important in the eventual identification of 1,2-DFBZ…HCCH complex lines. This spectrum was used to simplify the original 1,2-DFBZ/HCCH scan by removing transitions appearing in the second 1,2-DFBZ-only spectrum from the original scan containing both dimer components. (Once the spectrum was assigned, the strongest transitions were observable in the original EIU data set, but at very low signal-to-noise (S/N) ratio.)

DCCD was synthesized by reaction of D_2O (99.8 atom% D, Acros Chemical) on calcium carbide (80%, Aldrich) under vacuum. The resulting DCCD was condensed at liquid nitrogen temperature and later used to prepare a sample of 1% each of 1,2-DFBZ and DCCD diluted in He/Ne as before; transitions were initially identified using the EIU CP-FTMW spectrometer, and then the rotational spectrum was measured on the resonant cavity instrument. Presence of two quadrupolar D nuclei with unresolved hyperfine splitting led to messy transitions for which

average frequencies were fitted but the enriched sample provided sufficient intensity to be able to clearly assign the transitions using the CP-FTMW instrument. Some transitions for the two 1,2-DFBZ…$H^{13}C^{12}CH$ species (~1% natural abundance) were initially identified in the UVa broadband scan and their spectra were later measured on the resonant cavity instrument using an enriched isotopic sample (99.2% ^{13}C, CDN Isotopes). ^{13}C substitutions on the 1,2-DFBZ ring (~2% natural abundance by symmetry) were assigned entirely from the broadband scan.

3. Results and Discussion

3.1 Ab initio calculations

Both a non-planar form (with HCCH located above the aromatic ring, similar to BZ…HCCH and FBZ…HCCH dimers) and a planar form (with HCCH interacting simultaneously with a fluorine and hydrogen atom of difluorobenzene) were considered as possible structures for the 1,2-DFBZ…HCCH complex. The planar form is significantly higher in energy than the non-planar form (Table 1 and Electronic Supplementary Information (ESI) Table S1), with the energy difference ranging from *ca*. 200 to 660 cm^{-1}, depending on level and basis; the largest energy differences are encountered at the MP2 BSSE uncorrected level. In light of this large stability difference between non-planar and planar forms, spectroscopic parameters for the planar form are listed only in Table S1, and that structure will be considered no further since inspection of fitted experimental rotational constants and planar moments immediately eliminates it as a possibility. Rotational constants and dipole moment components resulting from MP2, M06-2X and ωB97X-D optimizations with the different basis sets will be compared. Both BSSE uncorrected and corrected optimizations are listed in Table 1 for MP2 calculations, while only BSSE corrected results are given for DFT models. Figure 1 shows the

ωB97X-D/aug-cc-pVDZ optimized structures (BSSE corrected) for both non-planar and planar forms.

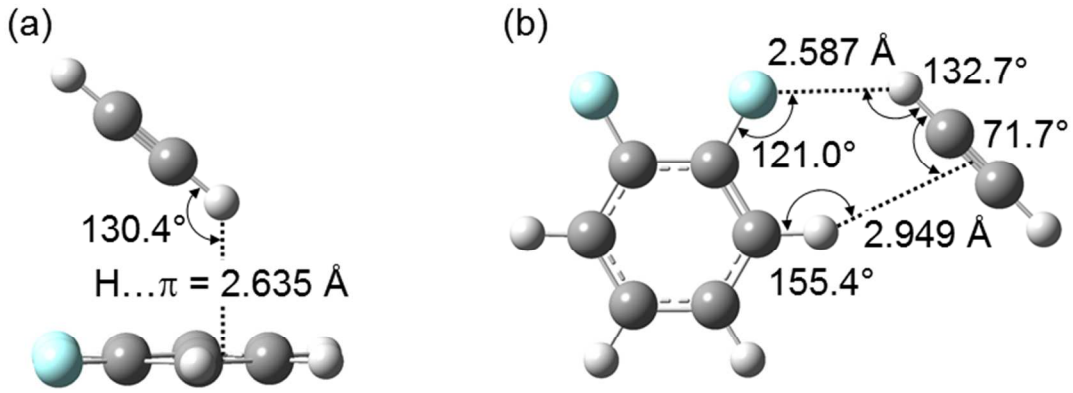

Figure 1 ωB97X-D/aug-cc-pVDZ predicted structures for (a) non-planar and (b) planar forms of 1,2-DFBZ…HCCH. These structures were obtained from BSSE corrected optimizations in which the planar form is predicted to be less stable than the non-planar form by 218 cm^{-1}.

For the non-planar form (Figure 1(a)), a significant variation in tilt angle of HCCH was observed depending on method and basis, with the angle between the C_2 axis of 1,2-DFBZ and the HCCH axis ranging from *ca*. 30° to 55° in our optimizations (last line of Table 1). This leads to a wide range of ratios of μ_a to μ_b dipole moment components (Table 1). Table 1 also reveals that the aug-cc-pVDZ basis tends to yield less compact structures (with smaller rotational constants) in all cases. BSSE uncorrected MP2 calculations with Pople basis sets predict almost identical μ_a and μ_b values (predicted *b*-type:*a*-type spectral intensity ratio = 1.02), while correction for BSSE makes the *b*-type transitions relatively more intense (predicted *b*-type:*a*-type intensity = 2.8), highlighting the sensitivity of these optimizations to inclusion of BSSE corrections. Interestingly, most theoretical methods give similar results with the two different basis sets, but the MP2 BSSE uncorrected results that go from predicting equal intensity *a*- and *b*- type transitions (6-311++G(2d,2p) basis) to *b*-types being a factor of 12 more intense (aug-cc-pVDZ basis) seem to be a dramatic exception to this trend.

3.2 Rotational spectra

Initial attempts to assign the spectrum focused on searching for quartets of transitions with characteristic closed loop patterns arising from shared rotational levels (e.g. $4_{04}\leftarrow3_{13}$, $4_{14}\leftarrow3_{13}$, $4_{04}\leftarrow3_{03}$, $4_{14}\leftarrow3_{03}$), with initial MP2/6-311++G(2d,2p) predictions suggesting *a*- and *b*-type transitions should have similar intensity (μ_a = 1.64 D, μ_b = 1.66 D, Table 1).

An intense and quite rich monomer spectrum[30] and transitions for 1,2-DFBZ dimer[31] and 1,2-DFBZ…H_2O[32] led to the original (6 – 20 GHz) spectral scan being quite dense, with in excess of 7,000 transitions at or above a signal to noise level of 2 (giving an average spectral line density of around 1 line every 2 MHz). The noise level in this scan was close to 1 μV. Two spectra separated by a few hundred megahertz, with approximately the expected closed loop patterns and intensity ratios predicted by the MP2 calculations, and with the spectrum offset to lower frequency being less intense, were found after a painstaking analysis, but significant difficulties were encountered in the fitting process and in explaining the apparent spectral doubling. The later broadband scan using a sample of only 1,2-DFBZ in Ne, and application of the spectral subtraction capability in the AABS spectral viewer/assignment package,[33] revealed that the spectrum we initially believed to be 1,2-DFBZ…HCCH was actually present in both scans, and what initially looked like two tunneling states are consistent with the isotopic shift expected upon substitution of ^{20}Ne with ^{22}Ne; zero point effects[34] are likely responsible for the larger than expected intensity of the lower abundance (~9%) ^{22}Ne isotope. The rotational constants of 1,2-DFBZ…Ne are predicted to be remarkably similar to those of 1,2-DFBZ…HCCH, helping to explain our initial confusion about the spectral carrier. Analysis of 1,2-DFBZ…Ne is still ongoing and will be reported separately.

Table 1 Ab initio (MP2) and density functional theory (M06-2X and ωB97X-D) predicted rotational constants and dipole moment components for the non-planar form of 1,2-DFBZ…HCCH. Both BSSE uncorrected and corrected results are presented for the MP2 calculations while only results from BSSE corrected results are given for DFT optimizations.

	MP2 (BSSE uncorrected)		**MP2 (BSSE corrected)**	
	6-311++G(2d,2p)	aug-cc-pVDZ	6-311++G(2d,2p)	aug-cc-pVDZ
A / MHz	1367.9	1283.6	1325.1	1316.7
B / MHz	1167.1	1125.2	1138.9	1122.6
C / MHz	1025.9	958.2	981.0	974.4
μ_a / D	1.64	0.68	1.20	1.40
μ_b / D	1.66	2.36	2.02	1.96
μ_c / D	0.00	0.00	0.00	0.00
$\left(\frac{\mu_b^2}{\mu_a^2}\right)$ [a]	1.02	12.0	2.83	1.96
θ / degrees[b]	32	50	33	31
	DFT (BSSE corrected)			
	M06-2X/ 6-311++G(2d,2p)	M06-2X/ aug-cc-pVDZ	ωB97X-D/ 6-311++G (2d,2p)	ωB97X-D/ aug-cc-pVDZ
A / MHz	1371.0	1337.8	1318.5	1306.2
B / MHz	1162.8	1148.1	1111.8	1105.3
C / MHz	1016.6	987.4	952.1	946.8
μ_a / D	1.56	1.28	0.75	0.80
μ_b / D	1.81	2.04	2.24	2.25
μ_c / D [c]	0.00	0.07	0.04	0.00
$\left(\frac{\mu_b^2}{\mu_a^2}\right)$ [a]	1.35	2.54	8.92	7.91
θ / degrees[b]	32	35	41	39

[a] Predicted ratio of intensities of *b*-type to *a*-type transitions.
[b] The parameter θ gives the tilt angle of the HCCH; i.e. the angle between the HCCH axis and the C_2 axis of difluorobenzene.
[c] Although by symmetry the μ_c component would be exactly zero, no symmetry restrictions were imposed during the optimization process leading to some slightly non-zero values of this parameter.

Once transitions present in the 1,2-DFBZ/Ne spectrum were subtracted from the scan, patterns belonging to the 1,2-DFBZ…HCCH spectrum were located, with *b*-type transitions several times more intense than *a*-types (see Figure 2), in line with ωB97X-D predictions (Table 1). After initial assignment, it was relatively straightforward to locate and fit all parent isotopologue transitions within the broadband spectrum using the AABS software[33] interfaced with the SPFIT/SPCAT package of Pickett.[35] Spectra were fitted to a Watson *A* reduction Hamiltonian[36] in the I^r representation, with resulting spectroscopic parameters listed in Table 2. All five quartic centrifugal distortion constants and some sextic terms were required for a satisfactory fit (with the particular choice of sextic terms being decided by an empirical process whereby only constants that were well determined and that had a noticeable effect on the $\Delta\nu_{rms}$ were included in the fit). Fitted transition frequencies for all isotopologues are given in ESI Table S2. Attempts to fit to a Watson *S* reduction resulted in a significantly higher $\Delta\nu_{rms}$ value as expected for such an asymmetric species ($\kappa \sim -0.16$).

The spectral line density made ^{13}C assignments challenging due to many possible options with similar intensity for each transition. The spectrum for the carbon substitution with the largest change in rotational constants ($^{13}C_{13}$) was assigned last and was successfully identified using an AUTOFIT routine[37] after predicted isotopic rotational constants had been refined based on planar moment variations observed for the other ^{13}C species. The weakness of ^{13}C transitions, leading to smaller than usual data sets, means that deviations in the fits (Table 2) are larger than typical.

Table 2 Fitted spectroscopic parameters for the 1,2-DFBZ…HCCH dimer. See Figure 3 for atom numbering.

Parameter [a]	Normal	$^{13}C_1$	$^{13}C_2$	$^{13}C_3$	$^{13}C_{12}$	$^{13}C_{13}$	DCCD
A / MHz	1316.31232(14)	1304.4550(16)	1308.5818(11)	1313.6722(16)	1313.1285(18)	1316.3461(15)	1306.5907(14)
B / MHz	1097.62717(13)	1093.0948(12)	1091.2481(8)	1095.8880(9)	1082.648(5)	1070.6284(9)	1048.4336(20)
C / MHz	940.61733(15)	932.7860(12)	938.7425(8)	939.6319(10)	928.0688(9)	920.6693(9)	899.8341(19)
Δ_J / kHz	4.7664(34)	4.595(14)	4.710(11)	4.730(14)	4.592(7)	4.842(15)	4.55(4)
Δ_{JK} / kHz	19.095(5)	19.45(7)	18.84(5)	19.06(9)	18.43(18)	19.13(7)	14.43(14)
Δ_K / kHz	–22.508(7)	–22.37(6)	–22.13(4)	–22.43(8)	–22.16(18)	[–22.508]	–18.13(10)
δ_J / kHz	0.1117(5)	[0.1117][b]	[0.1117]	[0.1117]	[0.1117]	[0.1117]	0.304(15)
δ_K / kHz	5.605(8)	6.20(11)	5.51(7)	[5.605]	[5.605]	[5.605]	[5.605]
ϕ_J / Hz	–0.405(29)	[–0.405]	[–0.405]	[–0.405]	[–0.405]	[–0.405]	[–0.405]
ϕ_K /Hz	4.48(31)	[4.48]	[4.48]	[4.48]	[4.48]	[4.48]	[4.48]
$\Delta\nu_{rms}$ / kHz [c]	1.8	7.2	6.0	7.2	3.7	4.9	4.0
N [d]	83	19	23	19	14	17	13
P_{cc} / u Å^2 [e]	153.53988(9)	153.9840(8)	155.4832(6)	154.0093(7)	153.5582(16)	153.5198(7)	153.5944(13)

[a] Uncertainties in parentheses correspond to one standard deviation in the fitted parameters.

[b] Parameters in [ ] were fixed at values obtained for the parent isotopologue.

[c] $\Delta\nu_{\mathrm{rms}} = \left[\frac{\sum(\nu_{\mathrm{obs}}-\nu_{\mathrm{calc}})^2}{N}\right]^{\frac{1}{2}}$.

[d] Number of fitted rotational transitions; this includes both resonant cavity and broadband data. Since repeated measurements from both spectrometers have been shown to agree to within ±4 kHz, this is used as the uncertainty in all fitted transitions.

[e] Planar moment $P_{cc} = 0.5(I_a + I_b - I_c) = \sum_i m_i c_i^2$, etc.

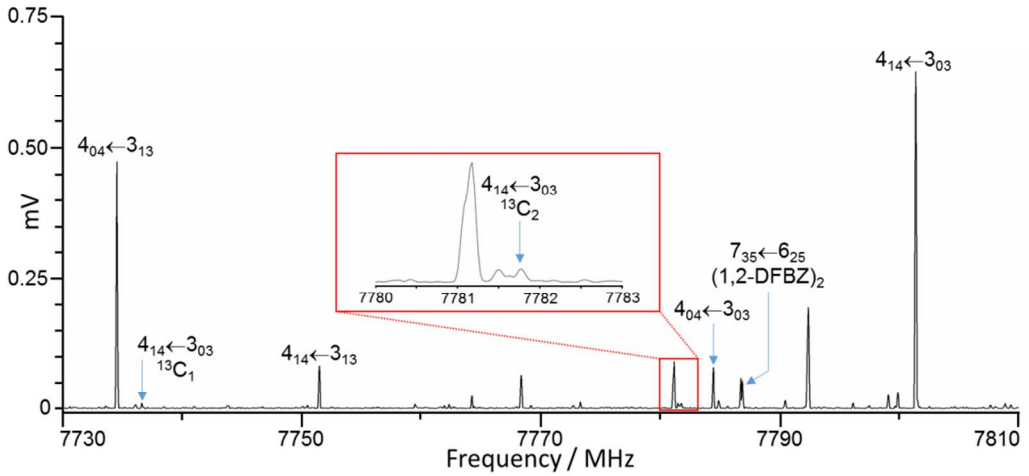

Figure 2 Section of broadband spectrum showing one of the quartets belonging to 1,2-DFBZ…HCCH. Also visible are transitions from ^{13}C substitutions on the ring ($^{13}C_1$ and $^{13}C_2$, see Figure 3) as well one of the closely spaced doublets belonging to the 1,2-DFBZ dimer.[31]

3.3 Structure determination and binding

The fact that HCCH lies in the symmetry plane bisecting the two fluorine atoms of difluorobenzene can be confirmed by comparison of the P_{cc} planar moment of the dimer (P_{cc} = $0.5(I_a + I_b - I_c) = \Sigma_i\, m_i c_i^2$ = 153.53988(9) u Å^2, Table 2) with P_{bb} of 1,2-difluorobenzene monomer (154.8787(13) u Å^2).[30] The similarity of these two planar moments indicates that HCCH lies within the symmetry plane of the weak complex and that experimental rotational constants of the complex are not significantly contaminated by vibrational averaging from out of plane motions of HCCH within the dimer. In addition, small (~0.5 to 1.5 u Å^2) increases for ^{13}C substitutions of the ring carbons of difluorobenzene ($^{13}C_{1,2,3}$, see Figure 3 for atom numbering) confirm that these atoms lie outside of the *ab* symmetry plane, while P_{cc} values nearly identical to the parent isotopologue (within ~0.05 u Å^2) are observed for substitutions within the *ab* symmetry plane (carbon atoms of acetylene, $^{13}C_{12,13}$ and the DCCD species).

Precise intermolecular structural parameters for 1,2-DFBZ...HCCH were determined from rotational constants of the normal, five singly substituted ^{13}C isotopologues, and the DCCD

species following two complementary approaches: first, Kraitchman's single substitution equations[38] were used to determine principal axis coordinates for each carbon atom within the dimer (r_s, substitution structure), and then rotational constants of all isotopologues (Table 2) were used together in a least-squares fitting process to determine relative orientations of the two monomers with respect to each other (r_0, average structure).

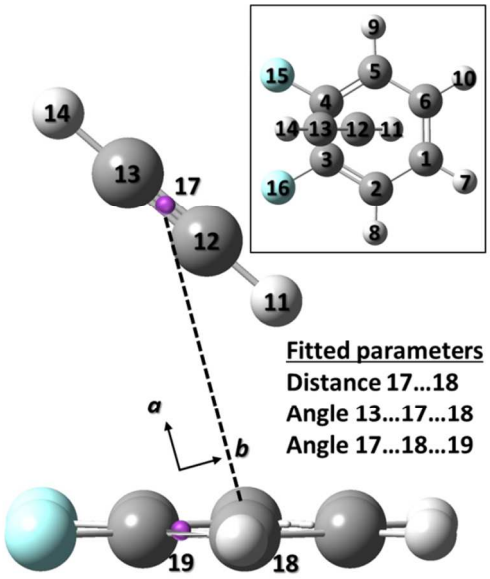

Figure 3 Atom numbering scheme and fitted parameters for the 1,2-difluorobenzene…acetylene complex. Dummy atom 17 marks the center of mass of acetylene, 18 the midpoint of the line between the C_2 and C_5 atoms and 19 the center of mass of difluorobenzene (points 18 and 19 then define the C_2 axis of difluorobenzene). The inset shows ring atom numbering. The *a* and *b* principal axes are also shown.

Principal axis coordinates of all substituted atoms, resulting from the r_s fit using Kisiel's KRA program,[39] are given in Table 3, along with r_0 (see below) and *ab initio* values for comparison. The substitution and inertial fit coordinates generally agree to about ±0.03 Å, with a few larger discrepancies, particularly in smaller values (for instance, the *b* coordinate of C_{13}), where the nature of Kraitchman's equations leads to unreliable results. For 1,2-DFBZ...HCCH, *ab initio* calculations have revealed a relatively flat potential energy surface for rotation of

HCCH about its center of mass while it remains in the (*ab*) symmetry plane of the dimer (see above). This could be an indication that HCCH is able to undergo relatively large amplitude low frequency vibrational motion within the complex, which would explain additional larger than expected deviations (outside of reported Costain uncertainties[40]) between r_0 and r_s coordinates. Inclusion of two sextic centrifugal distortion constants in the spectroscopic fit (Table 2) is further suggestion that some vibrational motion may be present within this dimer. Finally, as confirmation of the isotopic assignments, r_s carbon framework geometries for the two monomers can be compared with literature values. The small *b*-coordinate (~0.1 Å) for C_{13} (Table 3) leads to a large discrepancy in the position of that atom, giving a much longer than reasonable C≡C bond;[41] however, the 1,2-DFBZ framework agrees reasonably well with the literature structure (Table 4).[42] The discrepancy in C_{13} position is likely also responsible for the large differences between r_0 and r_s structures reported in Table 5.

Table 3 Comparison of coordinates (Å) of isotopically substituted carbon atoms from r_s (substitution structure), r_0 (inertial fit of I_a and I_c) and r_e (ωB97X-D/aug-cc-pVDZ) results. [a)]

		a	*b*	*c*
C_1	$\|r_s\|$	1.187(1)	1.760(10)	0.684(2)
	r_0	–1.235(19)	1.703(11)	–0.696(0)
	r_e	–1.139	1.753	–0.701
C_2	$\|r_s\|$	0.859(2)	0.567(3)	1.403(1)
	r_0	–0.888(6)	0.544(8)	–1.401(0)
	r_e	–0.842	0.584	–1.401
C_3	$\|r_s\|$	0.510(3)	0.550(3)	0.688(2)
	r_0	–0.550(6)	–0.586(4)	–0.688(0)
	r_e	–0.562	–0.576	–0.700
C_{12}	$\|r_s\|$	2.510(10)	0.996(2)	0.000(12)
	r_0	2.471(2)	1.081(31)	0.000(0)
	r_e	2.473	0.994	0.018
C_{13}	$\|r_s\|$	3.4169(4)	0.109(14)	0.000(12)
	r_0	3.447(11)	0.378(16)	0.000(0)
	r_e	3.443	0.275	0.014

[a)] Atom numbering refers to Figure 3. *Ab initio* structure was optimized without symmetry constraints. r_e coordinates of ring atoms that should be equivalent to C_1, C_2 and C_3, respectively, are C_6 (–1.151, 1.749, 0.694), C_5 (–0.868, 0.579, 1.397), and C_4 (–0.575, –0.579, 0.692).

Table 4 Literature structures for 1,2-difluorobenzene[42] and HCCH[41] monomers. [a)]

1,2-difluorobenzene	Literature Values	r_s structure [b)]
C_3–C_4 / Å	1.3755(3)	1.3768(31)
C_2–C_3 / Å	1.3786(3)	1.3708(35)
C_1–C_2 / Å	1.4004(3)	1.4313(27)
C_1–C_6 / Å	1.3917(6)	1.3681(32)
C_2–C_3–C_4 / °	121.17(2)	121.42(23)
C_1–C_2–C_3 / °	118.59(2)	118.39(15)
C_2–C_1–C_6 / °	120.24(1)	120.15(12)
C_3–F_{15} / Å	1.3494(4)	--
C_2–H_8 / Å	1.0829(1)	--
C_1–H_7 / Å	1.0813(4)	--
F_{15}–C_3–C_4 / °	119.16(1)	--
H_8–C_2–C_3 / °	119.58(1)	--
H_7–C_1–C_2 / °	119.55(1)	--
HCCH		
C≡C / Å	1.203(2)	1.269(10)
C–H / Å	1.061(2)	--

[a)] Atom numbers refer to Figure 3. Structure of 1,2-DFBZ from ref. 42 is an r_s structure and the structure of HCCH from ref. 41 is an r_e structure.
[b)] Derived from r_s coordinates reported in Table 3 using signs from corresponding r_0 coordinates.

Intermolecular structural parameters derived from substitution coordinates using Kisiel's EVAL program[39] are compared with results of a series of least-squares fits of structural

parameters to the moments of inertia of all assigned isotopologues in Table 5. If it is assumed that monomer structures are unchanged from literature values (Table 4),[41,42] and that HCCH lies in the symmetry plane that bisects the 1,2-DFBZ ring, then there are three intermolecular structural parameters to be determined. For inertial fits, performed using Kisiel's STRFIT program,[43] these were chosen as the distance between the HCCH triple bond center (X_{17}, X = dummy atom) and a point lying on the C_2 axis of difluorobenzene, centered between C_2 and C_5 (designated X_{18}), and the angles C_{13}–X_{17}…X_{18} and X_{17}…X_{18}–X_{19} (where X_{19} is the center of mass of 1,2-DFBZ). Inertial fits of pairs of moments of inertia resulted in lower RMS values than the fit of all three moments of inertia, since the adjustable intermolecular parameters lie completely within the symmetry plane of the dimer (thus the variable part of the structure is essentially "planar"). The structure derived from a fit of I_a and I_c is favored, since it leads to the lowest RMS deviation of fitted moments of inertia; principal axis coordinates for this structure (and the best computational structure) are listed in Tables S3 and S4.

Table 5 Comparison of results of least-squares fits of intermolecular structural parameters when different combinations of moments of inertia are fitted. The preferred result is that derived by fitting I_a and I_c, since it gives the smallest rms deviation of fitted moments. See Figure 3 for atom numbers.

	r_0				r_s [b]	r_e [c]
	$I_aI_bI_c$	I_aI_b	I_aI_c	I_bI_c		
Fitted Parameters						
$R_{17\text{-}18}$ / Å	3.8426(59)	3.8363(18)	3.8515(20)	3.8402(31)	3.8227(18)	3.814
$\theta_{17\text{-}18\text{-}19}$ / °	76.48(45)	76.42(14)	76.08(15)	76.94(24)	72.43(20)	76.9
$\theta_{13\text{-}17\text{-}18}$ / °	142.7(3.7)	144.4(1.2)	141.5(1.3)	141.8(1.7)	135.8(1.1)	142.6
Derived Parameters						

$R_{17\text{-}19}$ (R_{cm})/ Å	3.739(24)	3.7324(75)	3.7429(82)	3.743(11)	3.717
$\theta_{13\text{-}17\text{-}19}$ / °	131.5(8.2)	133.2(2.6)	130.4(2.6)	130.7(4.4)	131.2
$\theta_{17\text{-}19\text{-}18}$ / °	92.4(2.6)	92.4(8)	92.8(9)	91.9(1.4)	91.7
C_{12}–H_{11}···π / Å [a)]	2.687(64)	2.643(20)	2.725(28)	2.701(30)	2.635
RMS / u Å^2	0.597	0.164	0.154	0.205	–

[a)] Perpendicular distance to the aromatic ring plane from the nearest HCCH hydrogen atom.
[b)] Derived from r_s coordinates reported in Table 3 using signs from corresponding r_0 coordinates. The large differences between the r_s and r_0 structures likely arise from one or more small r_s coordinates, leading to some structural parameters being unreliable.
[c)] ωB97X-D/aug-cc-pVDZ.

Although r_0 and r_s intermolecular parameters do not agree well with each other, this likely arises mainly from the large discrepancy (possibly up to ~0.1 – 0.2 Å) in the *b* coordinate of atom C_{13} in the r_s structure, as discussed above (Table 3). The best *ab initio* structure, calculated at ωB97X-D/aug-cc-pVDZ level, is in excellent agreement with r_0 results, with most intermolecular distances agreeing to within ~0.04 Å and angles to within ~1° (although the theoretical C–H...π distance is nearly 0.1 Å shorter than the observed value) explaining the good agreement between predicted and experimental rotational constants (Tables 1 and 2) for the parent isotopologue, equivalent to performance of MP2/6-311++G(2d,2p) methods for similar species in the past.[4,5]

It has been shown[43,44] that inclusion of Watson's c_α and d_α, and/or Laurie's δ_H, parameters, resulting in r_m geometries,[45] can improve inertial fit quality when significant vibrational effects are present from large intermolecular motions or deuterium substitutions. A series of fits was performed in which various combinations of these parameters were included. Although it was possible to make small improvements in resulting RMS deviations (compared to fits without these parameters), the additional constants were poorly determined in all cases, and

uncertainties in derived structural parameters were typically as large, or larger, than in the traditional r_0 fits. We feel that the simple r_0 fits, including only intermolecular parameters as variables, provide the best possible structure for this dimer, and therefore only results of these successful inertial fits are presented (Table 5).

3.4 Comparison with related complexes

This is the third dimer in a series of substituted benzenes with acetylene that has recently been investigated using rotational spectroscopy, and comparison with BZ…HCCH[4] and FBZ…HCCH,[5] particularly focusing on the variation in weak CH…π interactions, is presented below.

The most obvious difference between 1,2-DFBZ…HCCH and the benzene and fluorobenzene complexes is that in the previous two dimers HCCH lies perpendicular or nearly perpendicular to the aromatic ring plane, while in 1,2-DFBZ…HCCH the axis of HCCH is significantly tilted away from perpendicular to the ring (Table 6). The benzene complex has average C_{6v} symmetry, while for fluorobenzene, the axis of HCCH tilts about 7° away from perpendicular, with the hydrogen atom nearest the ring moving away from the fluorine atom. For the present dimer, the HCCH axis tilts 46(3)° from perpendicular, again with the hydrogen atom nearest the ring moving away from the fluorine atoms. The tilt of acetylene away from perpendicular as the degree of fluorination increases is likely due to the electron withdrawing effect of the fluorine atoms, thus requiring the slightly acidic hydrogen atom to tilt toward the more electron rich part of the aromatic ring to maintain the best electrostatic interaction. The attraction between HCCH and the aromatic π electrons also becomes weaker as fluorine atoms are added to the ring (see below). Possible weakening of the HCCH...π interaction as degree of

ring fluorination increases is reflected in the CH...π distances in the three complexes (Table 6). Although the fluorobenzene and benzene complexes have virtually identical H...π distances (2.492 Å), the distance in the 1,2-DFBZ complex is significantly longer (2.725(28) Å). The reason for acetylene tilting rather than remaining perpendicular to the ring while moving away from the F atoms is unclear, but is likely related to maximized dispersion and/or electrostatic interaction terms involving higher order multipole moments.

Table 6 Comparison of intermolecular parameters and binding energies for complexes of aromatic molecules with HCCH.

	1,2-Difluorobenzene	Fluorobenzene5	Benzene4
C_{12}–H_{11}...π / Å [a)]	2.725(28)	2.492(47)	2.4921(1)
Deviation from ⊥ / ° [b)]	46(3)	7(3)	0
k_s / N m^{-1}	2.0(3)	2.8(6)	4.9(5)
E_B / kJ mol^{-1}	2.3(6)	4.1(8)	7.1(7)

[a)] Perpendicular distance to the aromatic ring plane from the nearest HCCH hydrogen atom.
[b)] Angle between HCCH axis and an axis normal to the aromatic ring plane.

If the *a*-axis of the dimer lies approximately along the intermolecular bond (a good approximation in the present case, see Figure 3), a pseudodiatomic model may be used to estimate the binding energy (E_B) and weak bond stretching force constant (k_s) for the interaction, as given by equations (1) and (2).[46,47]

$$k_s = \frac{16\pi^4(\mu R_{cm})^2\left[4B^4+4C^4-(B-C)^2(B+C)^2\right]}{hD_J} \quad (1)$$

$$E_B = \frac{1}{72}k_s R_{cm}^2 \quad (2)$$

In the above expressions, μ, R_{cm} and D_J are the reduced mass, center of mass separation and Watson *S* reduction centrifugal distortion constant, respectively. D_J (1.81 kHz) was calculated from Δ_J and δ_K using the relationship given in equation (4) of reference 19. This yields k_s = 2.0(3) N m^{-1} and E_B = 2.3(6) kJ mol^{-1}. Comparison with similarly obtained values for BZ…HCCH4 and FBZ…HCCH5 (Table 6) suggests that the interaction weakens as the level of fluorination increases along this series, with decreases in E_B of ~43-44% upon addition of each fluorine atom to the ring. Estimated binding energies computed using BSSE corrected dimer

energies from ωB97X-D/aug-cc-pVDZ optimized structures for these three complexes are somewhat higher but follow the same decreasing trend as fluorination increases (E_B = 12.4, 11.2 and 10.9 kJ mol^{-1} for BZ, FBZ and 1,2-DFBZ complexes of HCCH, respectively). These values compare favorably with symmetry adapted perturbation theory (SAPT)[48] interaction energies obtained from preliminary results at the MP2/aug-cc-pVDZ level with the SAPT2012 program[49] which give values of 12.2, 10.5 and 9.9 kJ mol^{-1} for BZ, FBZ and 1,2-DFBZ…HCCH respectively. These calculations utilized the dimer centered basis set and GAMESS[50] was used as the *ab initio* package. Interestingly, although monomer dipole moments increase dramatically from BZ (0 D) to FBZ (1.555(3) D)[51] to 1,2-DFBZ (2.59(2) D),[30] seemingly in contrast to the trend in E_B, the computed out of plane components of the monomer quadrupole moments (ωB97X-D/6-311G**)[52] decrease by ~25-27% as each F atom is added (BZ = –8.2 D Å, FBZ = –6.1 D Å, 1,2-DFBZ = –4.4 D Å); thus, the decrease in binding energy along the series may reflect a subtle interplay of dipole-quadrupole and quadrupole-quadrupole interactions.

4. Conclusion

The 1,2-difluorobenzene…HCCH complex continues the series of structural studies of aromatic molecules complexed with acetylene. In the present case the H…π distance is significantly longer than it has been in the other two members of the series and the binding energy, as estimated by the pseudodiatomic model, is the weakest of the three complexes yet studied. This contrasts with the fact that 1,2-DFBZ is the most polar aromatic studied so far in this series. Future studies of the effectiveness of DFT levels applied to these fluorinated species would be of interest, particularly in light of differences in the various contributions to the interaction energy (ranging from a dispersion interaction between the two non-polar entities in

the BZ…HCCH complex to contributions from electrostatic interactions in complexes of HCCH with the increasingly polar FBZ and DFBZ). Future work will focus on whether changing the position of fluorination from 1,2-difluorobenzene to 1,3-difluorobenzene or adding more fluorine atoms to the ring (e.g. 1,2,3-trifluorobenzene) changes the strength or structural aspects of the interactions with HCCH. It is also hoped that these experimental studies will prompt more thorough theoretical investigations of the interactions in this series of fluorinated benzenes with HCCH, particularly in terms of quantifying the balance of forces responsible for the binding. Further studies applying SAPT to these systems will aim to quantify and contrast the varying contributions to the overall interaction energy. Such calculations may also help to better understand the reason for the tilt of acetylene away from perpendicular to the aromatic ring.

Acknowledgments

This work was supported by National Science Foundation Research at Undergraduate Institutions grants CHE-1214070 (EIU student support) and CHE-0809387 (EIU instrument construction) and grants CHE-09600741 (UVa instrument) and CHE-1213200 (UVa research support). The authors thank Prof. Heinrich Maeder for supplying data on 1,2-DFBZ…H_2O. Erica Webster performed the original synthesis of DCCD and Prof. Robert Kuczkowski provided ^{13}C-enriched acetylene used in this work. William C. Trendell is acknowledged for providing interaction energy data from his SAPT calculations.

Table of Contents Graphic

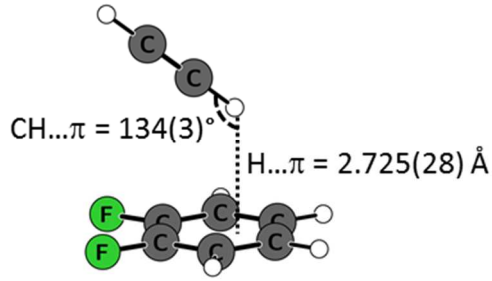

The H…π distance increases in o-$C_6H_4F_2$…HCCH, compared to C_6H_5F…HCCH or C_6H_6…HCCH, consistent with weaker interactions with increased ring fluorination.

References

[1] M. Nishio, *The CH/π Hydrogen Bond*, http://www.tim.hi-ho.ne.jp/dionisio/, accessed 5/13/2016.

[2] M. Kumar, P. Balaji, *J. Mol. Model.*, 2014, **20**, 2136.

[3] A. Barman, B. Batiste and D. Hamelberg, *J. Chem. Theory Comput.*, 2015, **11**, 1854.

[4] N. W. Ulrich, N. A. Seifert, R. E. Dorris, R. A. Peebles, B. H. Pate and S. A. Peebles, *Phys. Chem. Chem. Phys.*, 2014, **16**, 8886.

[5] N. W. Ulrich, T. S. Songer, R. A. Peebles, S. A. Peebles, N. A. Seifert, C. Pérez and B. H. Pate, *Phys. Chem. Chem. Phys.*, 2013, **15**, 18148.

[6] B. K. Mishra, S. Karthikeyan and V. Ramanathan, *J. Chem. Theory Comput*., 2012, **8**, 1935.

[7] S. Tsuzuki, and A. Fujii, *Phys. Chem. Chem. Phys.*, 2008, **10**, 2584.

[8] S. Tsuzuki, *Annu. Rep. Prog. Chem., Sect. C: Phys. Chem.*, 2012, **108**, 69.

[9] M. Majumder, B. K. Mishra and N. Sathyamurthy, *Chem. Phys. Lett.*, 2013, **557**, 59.

[10] P. Tarakeshwar, K. S. Kim, E. Kraka and D. Cremer, *J. Chem. Phys.*, 2001, **115**, 6018.

[11] C. Calabrese, Q. Guo, A. Maris, W. Caminati, S. Melandri, *J. Phys. Chem. Lett.*, 2016, **7**, 1513.

[12] S. Schlücker, R. K. Singh, B. P. Asthana, J. Popp, W. Kiefer, *J. Phys. Chem. A*, 2001, **105**, 9983.

[13] A. Dkhissi, L. Adamowicz, G. Maes, *J. Phys. Chem. A*, 2000, **104**, 2112.

[14] A. Destexhe, J. Smets, L. Adamowicz, G. Maes, *J. Phys. Chem.*, 1994, **98**, 1506.

[15] F. A. Baiocchi, J. H. Williams and W. Klemperer, *J. Phys. Chem.*, 1983, **87**, 2079.

[16] W. G. Read, E. J. Campbell, G. Henderson, *J. Chem. Phys.*, 1983, **78**, 3501.

[17] S. A. Cooke, G. K. Corlett, C. M. Evans, A. C. Legon, *Chem. Phys. Lett.*, 1997, **272**, 61.

[18] M. E. Sanz, S. Antolínez, J. L. Alonso, J. C. López, R. L. Kuczkowski, S. A. Peebles, R. A. Peebles, F. C. Bowman, E. Kraka, D. Cremer, *J. Chem. Phys.*, 2003, **118**, 9278.

[19] K. Brendel, H. Mäder, Y. Xu and W. Jäger, *J. Mol. Spectrosc.*, 2011, **268**, 47.

[20] S. Suzuki, P. G. Green, R. E. Bumgarner, S. Dasgupta, W. A. Goddard, and G. A. Blake, *Science*, 1992, **257**, 942.

[21] H. S. Gutowsky, T. Emilsson and E. Arunan, *J. Chem. Phys.*, 1993, **99**, 4883.

[22] M. J. Frisch, G. W. Trucks, H. B. Schlegel, G. E. Scuseria, M. A. Robb, J. R. Cheeseman, G. Scalmani, V. Barone, B. Mennucci, G. A. Petersson, H. Nakatsuji, M. Caricato, X. Li, H. P. Hratchian, A. F. Izmaylov, J. Bloino, G. Zheng, J. L. Sonnenberg, M. Hada, M. Ehara, K. Toyota, R. Fukuda, J. Hasegawa, M. Ishida, T. Nakajima, Y. Honda, O. Kitao, H. Nakai, T. Vreven, J. J. A. Montgomery, J. E. Peralta, F. Ogliaro, M. Bearpark, J. J. Heyd, E. Brothers, K. N. Kudin, V. N. Staroverov, T. Keith, R. Kobayashi, J. Normand, K. Raghavachari, A. Rendell, J. C. Burant, S. S. Iyengar, J. Tomasi, M. Cossi, N. Rega, J. M. Millam, M. Klene, J. E. Knox, J. B. Cross, V. Bakken, C. Adamo, J. Jaramillo, R. Gomperts, R. E. Stratmann, O. Yazyev, A. J.

Austin, R. Cammi, C. Pomelli, J. W. Ochterski, R. L. Martin, K. Morokuma, V. G. Zakrzewski, G. A. Voth, P. Salvador, J. J. Dannenberg, S. Dapprich, A. D. Daniels, O. Farkas, J. B. Foresman, J. V. Ortiz, J. Cioslowski, D. J. Fox, J. A. Montgomery Jr., J. E. Peralta, F. Ogliaro, M. Bearpark, J. J. Heyd, E. Brothers, K. N. Kudin, V. N. Staroverov, R. Kobayashi, J. Normand, K. Raghavachari, A. Rendell, J. C. Burant, S. S. Iyengar, J. Tomasi, M. Cossi, N. Rega, J. M. Millam, M. Klene, J. E. Knox, J. B. Cross, V. Bakken, C. Adamo, J. Jaramillo, R. Gomperts, R. E. Stratmann, O. Yazyev, A. J. Austin, R. Cammi, C. Pomelli, J. W. Ochterski, R. L. Martin, K. Morokuma, V. G. Zakrzewski, G. A. Voth, P. Salvador, J. J. Dannenberg, S. Dapprich, A. D. Daniels, Ö. Farkas, J. B. Foresman, J. V. Ortiz, J. Cioslowski and D. J. Fox, *Gaussian 09, Revision C.01*, Gaussian, Inc., Wallingford, CT, 2010.

[23] Y. Zhao and D. G. Truhlar, *Theor. Chem. Acc.*, 2008, **120**, 215.

[24] J.-D. Chai and M. Head-Gordon, *Phys. Chem. Chem. Phys.*, 2008, **10**, 6615.

[25] S. F. Boys, and F. Bernardi, *Mol. Phys*. 1970, **19**, 553.

[26] D. A. Obenchain, A. A. Elliott, A. L. Steber, R. A. Peebles, S. A. Peebles, C. J. Wurrey and G. A. Guirgis, *J. Mol. Spectrosc.*, 2010, **261**, 35.

[27] G. G. Brown, B. C. Dian, K. O. Douglass, S. M. Geyer, S. T. Shipman and B. H. Pate, *Rev. Sci. Instrum.*, 2008, **79**, 053103.

[28] T. J. Balle and W. H. Flygare, *Rev. Sci. Instrum.*, 1981, **52**, 33.

[29] J. J. Newby, M. M. Serafin, R. A. Peebles and S. A. Peebles, *Phys. Chem. Chem. Phys.*, 2005, **7**, 487.

[30] L. Nygaard, E. Risby Hansen, R. Lykke Hansen, J. Rastrup-Andersen, G. O. Sorensen, *Spectrochim. Acta*, 1967, **23A**, 2813.

[31] T. Goly, U. Spoerel, W. Stahl, *Chem. Phys*. 2002, **283**, 289.

[32] K. Brendel Ph.D. Thesis, "Contributions to molecular beam Fourier Transform microwave spectroscopy: Experimental control, double resonance method, and investigations on the structure and dynamics of dimers of fluoridated benzenes with water" Christian-Albrechts-Universitaet zu Kiel, Kiel, Germany 2004

[33] Z. Kisiel, L. Pszczolkowski, I. R. Medvedev, M. Winnewisser, F. C. De Lucia, E. Herbst, *J.Mol.Spectrosc.*, 2005, **233**, 231.

[34] Y. Xu and W. Jäger, *Phys. Chem. Chem. Phys.*, 2000, **2**, 3549.

[35] H. M. Pickett, *J. Mol. Spectrosc.*, 1991, **148**, 371.

[36] J. K. G. Watson, in: J. R. Durig, (Ed.), *Vibrational Spectra and Structure*, Vol. 6, Elsevier, New York, 1977.

[37] N. A. Seifert, I. A. Finneran, C. Perez, D. P. Zaleski, J. L. Neill, A. L. Steber, R. D. Suenram, A. Lesarri, S. T. Shipman, B. H. Pate, *J. Mol. Spectrosc.*, 2015, **312**, 13.

[38] J. Kraitchman, *Am. J. Phys.*, 1953, **21**, 17.

[39] Kraitchman coordinates and structures from the KRA and EVAL code, Kisiel, Z. PROSPE− Programs for Rotational Spectroscopy. http://info.ifpan.edu.pl/~kisiel/prospe.htm (accessed June 2016).

[40] C. C. Costain, *J. Chem. Phys.*, 1958, **29**, 864.

[41] M. D. Harmony, V. W. Laurie, R. L. Kuczkowski, R. H. Schwendeman, D. A. Ramsay, F. J. Lovas, W. J. Lafferty and A. G. Maki, *J. Phys. Chem. Ref. Data*, 1979, **8**, 619.

[42] O. L. Stiefvater, *Z. Naturforsch.* 1988, **43a**, 147.

[43] Z. Kisiel, *J. Mol. Spectrosc.*, 2003, **218**, 58.

[44] Z. Kisiel, B. A. Pietrewicz, and L. Pszczołkowski, *J. Chem. Phys.* 2002, **117**, 8248.

[45] J. K. G. Watson, A. Roytburg, and W. Ulrich, *J. Mol. Spectrosc.* 1999, **196**, 102.

[46] D. J. Millen, *Can. J. Chem.* 1985, **63**, 1477.

[47] T.J. Balle, E.J. Campbell, M.R. Keenan, and W.H. Flygare, *J. Chem. Phys*. 1980, **72**, 922.

[48] B. Jeziorski, R. Moszynski, and K. Szalewicz, *Chem. Rev.*, 1994, **94**, 1887.

[49] R. Bukowski, W. Cencek, P. Jankowski, M. Jeziorska, B. Jeziorski, S. A. Kucharski, V. F. Lotrich, A. J. Misquitta, R. Moszynski, K. Patkowski, F. Rob, S. Rybak, K. Szalewicz, H. L. Williams, R. J. Wheatley, P. E. S. Wormer, and P. S. Żuchowski SAPT2012: An Ab Initio Program for Symmetry-Adapted Perturbation Theory Calculations of Intermolecular Interaction Energies, revision 2012.2. Department of Physics and Astronomy, University of Delaware, Newark, Delaware 19716 and Department of Chemistry, University of Warsaw ul. Pasteura 1, 02-093 Warsaw, 2012.

[50] M. W. Schmidt, K. K. Baldridge, J. A. Boatz, S. T. Elbert, M. S. Gordon, J. H. Jensen, S. Koseki, N. Matsunaga, K. A. Nguyen, S. Su, T. L. Windus, M. Dupuis, and J. A. Montgomery. *J. Comput. Chem*. 1993, **14**, 1347.

[51] R. A. Appleman, S. A. Peebles, and R. L. Kuczkowski, *J. Mol. Struct.*, 1998, **446**, 55.

[52] NIST Computational Chemistry Comparison and Benchmark Database, NIST Standard Reference Database Number 101, Release 17b, September 2015, Editor: Russell D. Johnson III, http://cccbdb.nist.gov/ Accessed May 2016.